FERMILAB-PUB-18-491-DI-TD
ACCEPTED

Thermal link design for conduction cooling of SRF cavities using cryocoolers

R. C. Dhuley, R. Kostin, O. Prokofiev, M. I. Geelhoed, T. H. Nicol, S. Posen, J. C. T. Thangaraj, T. K. Kroc, and R. D. Kephart

***Abstract*— Superconducting radio frequency (SRF) cavities with quality factors ~10^{10} near 4 K have potential to be cooled using regenerative-cycle cryocoolers. Contrary to using liquid helium, cryogen-free operation can be realized by conductively linking a cryocooler to a cavity for extracting the cavity RF dissipation. The cavity-cryocooler thermal link needs careful design as its thermal conductance will control the temperatures of the cavity and the cryocooler. We present a thermal analysis of a conduction-cooled SRF cavity that identifies the link thermal conductance requirement. The analysis uses published or expected RF dissipation characteristics of an Nb_3Sn coated niobium cavity and measured cooling capacity of a pulse tube cryocooler. We describe the mechanical design of a link that is constructed using commercial high-purity aluminum and facilitates bolted-connection to elliptical SRF cavities. The thermal performance of the link is assessed by finite element simulations, taking into account temperature dependent thermal conductivities and measured thermal contact resistance of aluminum and niobium. The link is shown to support operation at an accelerating gradient of 10 MV/m with the lowest-known 'perfect' Nb_3Sn residual surface resistance (~10 nΩ) and also under non-ideal cases that assume certain static heat leak into the system and non-perfect Nb_3Sn coatings.**

***Index Terms*—Cryogenics, particle accelerator, superconducting microwave devices, thermal analysis, thermal resistance.**

I. Introduction

THE cryogenic advantage of superconducting radio frequency (SRF) cavities with a thin internal coating of Nb_3Sn is evident for use in particle accelerators. The Nb_3Sn superconducting transition temperature of 18 K, which is almost twice that of pure niobium, presents relatively small 4K BCS resistance compared to niobium and to the expected Nb_3Sn residual resistance. Nb_3Sn coated 1.3 GHz cavities have in fact shown quality factors as high as 2x10^{10} in 4.2 K liquid helium and have sustained quality factors of ~10^{10} at gradients >10 MV/m [1]. The feasibility of operating coated cavities in 4.2 K liquid helium instead of 2 K He II can offer significant cost reduction and simplicity of the accelerator.

As 4 K operation is cryogenically efficient, an even simpler avenue is cooling Nb_3Sn coated cavities with 4 K regenerative cryocoolers *via* a thermal conduction link [2], [3], [4]. This conduction-cooling configuration can altogether remove liquid cryogens from the accelerator thereby streamlining its operation and also offering compactness. Although with another superconductor MgB_2, Holzbauer and Nassiri [5] and Nassiri *et al.* [6] have shown, *via* simulations, that such cryogen-free operation of coated cavities is feasible. Ciovati *et al.* [7] presented a design of a MW class cw SRF accelerator that uses Nb_3Sn coated cavities cooled by 4 K cryocoolers.

In the absence of liquid helium, the thermal link that connects a cavity to a cryocooler assumes the critical role of extracting RF heat dissipation from the cavity. The link must be carefully designed to have thermal conductance sufficient for balancing the cavity heat dissipation with the cryocooler capacity as well as to have easy mechanical integration with the cavity. In this paper, we discuss the general thermodynamic behavior of a SRF cavity-cryocooler system and outline a method for identifying the thermal conductance requirement. We present a link design that provides the required thermal conductance and offers a simple connection to the cavity. The design is based on the measured cooling capacity of a pulse tube cryocooler, heat dissipation processes in an SRF cavity, and some in-house characterized integration techniques that constitute the thermal link.

II. Thermal Link Design Methodology

A. RF cavity geometry and parameters

We consider niobium elliptical-cell cavities with the two common frequencies used for particle acceleration: 650 MHz and 1.3 GHz. We take that these accelerate relativistic electrons (β≈1 operation) with the net energy gain of 10 MeV. With an average accelerating gradient, E_{acc} of 10 MV/m over a length of 1 m, the 1.3 GHz cavity (TESLA style [8]) will comprise of 9 cells while the 650 MHz cavity (PIP-II style [9]) will be made up of 4.5 cells. We suppose further that these bulk niobium cavities are internally coated with Nb_3Sn. The coating can be grown following the tin vapor reaction procedure described in [1], which can yield residual surface resistance as small as 10 nΩ and E_{acc} > 10 MV/m with 4.2 K liquid helium.

This manuscript has been authored by Fermi Research Alliance, LLC under Contract No. DE-AC02-07CH11359 with the U.S. Department of Energy, Office of Science, Office of High Energy Physics. *(Corresponding author: R. C. Dhuley (rdhuley@fnal.gov))*

R. C. Dhuley, O. Prokofiev, M. I. Geelhoed, T. H. Nicol, S. Posen, J. C. T. Thangaraj, T. K. Kroc, and R. Kephart are with Fermi National Accelerator Laboratory, Batavia, IL 60510, USA. (emails: rdhuley@fnal.gov, prokofoe@fnal.gov, geelhoed@fnal.gov, tnicol@fnal.gov, sposen@fnal.gov, jtobin@fnal.gov, kroc@fnal.gov, kephart@fnal.gov)

R. Kostin is with Euclid Techlabs, LLC., Bolingbrook, IL 60440, USA. (email: r.kostin@euclidtechlabs.com)

Color versions of one or more of the figures in this paper are available online at http://ieeexplore.ieee.org.

Digital Object Identifier will be inserted here upon acceptance.

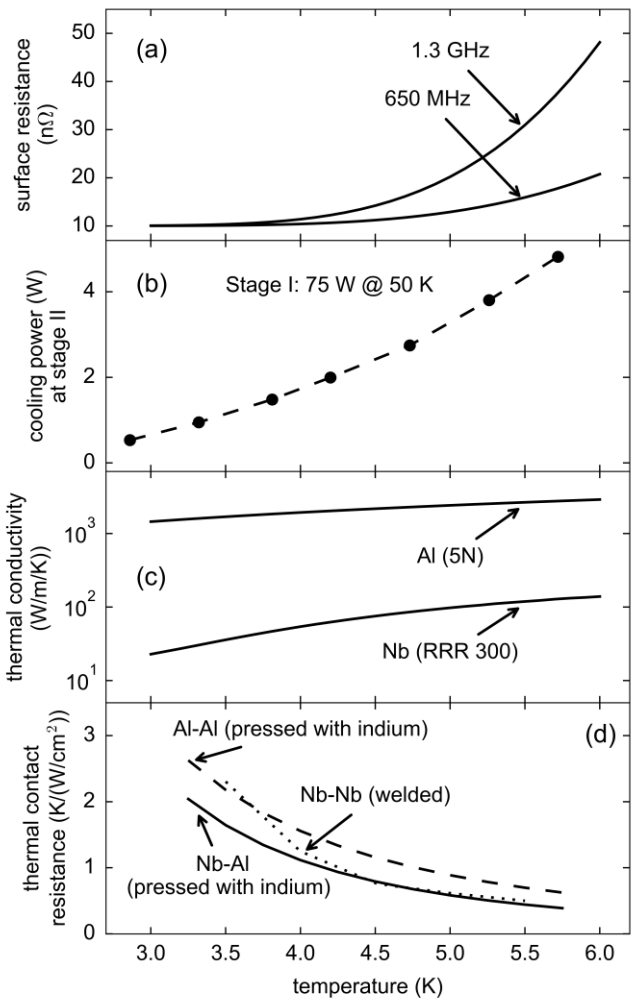

Fig. 1. Summary of material properties/cryocooler parameters used in the present analysis (a) RF surface resistance of Nb_3Sn calculated using SRIMP [10] for the BCS component and 10 nΩ residual resistance [1], (b) cooling capacity of Cryomech PT420 cryocooler stage II [14], as measured in-house, (c) thermal conductivity of 5N aluminum [11] and SRF grade niobium [12], and (d) thermal contact resistance of niobium-aluminum [13] and aluminum-aluminum bolted contacts, and thermal resistance of niobium-niobium electron-beam welds as measured in-house.

Fig. 1(a) shows the calculated surface resistance, R_s of Nb_3Sn assuming 10 nΩ residual resistance and temperature dependent BCS component obtained using SRIMP code [10]. At both 1.3 GHz and 650 MHz, the surface resistance near 4 K is dominated by the residual as BCS of Nb_3Sn is small at this temperature. The other cavity parameters relevant to dissipation, namely the geometry factor, G, accelerating length, L_{acc}, and normalized shunt impedance, R/Q are listed in Table I.

TABLE I
CAVITY PARAMETERS RELEVANT TO RF SURFACE DISSIPATION

Parameter*	650 MHz	1.3 GHz
G [Ω]	265	270
R/Q [Ω], per cell	150	115
L_{acc} [m], per cell	0.231	0.115

*G: cavity geometry parameter, R/Q: normalized shunt impedance, L_{acc}: effective accelerating length.

B. Thermodynamic behavior of cavity-thermal link-cryocooler system

A cryocooler conduction-cooled SRF system has three components: cavity- the heat source, cryocooler- the heat sink, and thermal link- the heat conduction medium. The cavity heat dissipation rate depends on the RF surface resistance and therefore on the temperature of the RF surface. The cryocooler cooling capacity is a function of the cryocooler temperature. A conduction-cooled SRF system therefore has a 'cyclic' dependency: the dissipation rate depends on the cavity temperature, the cavity temperature is dictated by the temperature rise across the link (*i.e.*, on its thermal conductance) and the cryocooler temperature, and the cryocooler temperature depends on the heat flow, *i.e.*, the cavity dissipation rate. Furthermore, the cooling link conductance will depend on the temperature distribution along its length (as thermal conductivity is highly temperature dependent near liquid helium temperature) and thus on the temperature at its two ends. Irrespective of this cyclic nature, same heat current will flow through the cavity-link-cryocooler chain at steady state. Therefore, the logical starting point of determining thermal conductance requirement is to apply the conservation of energy principle. At thermal steady state, conservation of energy will read:

$$(E_{acc}L_{acc})^2 * R_s(T_h)/(R/Q)/G = Q_c(T_c) = (T_h - T_c) * K_{link}(T_h, T_c), \quad (1)$$

where T_h and T_c are cavity and cryocooler temperature, R_s is RF surface resistance, Q_c is cryocooler cooling capacity, and K_{link} is thermal conductance of the link. The three terms from left to right in (1) represent cavity heat dissipation, cryocooler cooling power, and heat flow through the link, which must be equal at steady state.

Taking an initial estimate of T_h = 5 K, the 9-cell and 4.5-cell cavities will dissipate nearly 7.8 W of heat. For cooling the cavities, we select four cryocooler units, each rated to provide 2 W of cooling power at 4.2 K (Cryomech PT420) [14]. Fig. 1(b) displays the in-house measured cooling capacity *vs.* temperature at the 4 K stage of this cryocooler. We envision a thermal link that will attach to each cell of the cavity, extract the dissipated heat, and transport the heat to the four cryocoolers. We therefore will derive the link thermal conductance requirement based on power dissipation and available cooling *per cell*. For the 9-cell 1.3 GHz cavity, each cell will have available 4/9th of the total cooling capacity. Likewise, 4/4.5th of the total cooling power will be available for each cell of the 650 MHz cavity.

The necessary thermodynamic condition in addition to (1) is $T_h > T_c$ because the cavity (heat source) must run warmer than the cryocooler (heat sink). To determine the temperature regime where operation is possible, we plot T_h and T_c in Fig. 2(a) as a function of the heat flow from the cavity to the cryocooler. There clearly are three regimes in Fig. 2(a): $T_h < T_c$ (not physical), $T_h = T_c$ (not practical as this requires a link with infinite thermal conductance), and $T_h > T_c$ (physical). For the present case, 1.3 GHz and 650 MHz cavities require the cryocooler to operate warmer than 3.2 K and 3.8 K respectively.

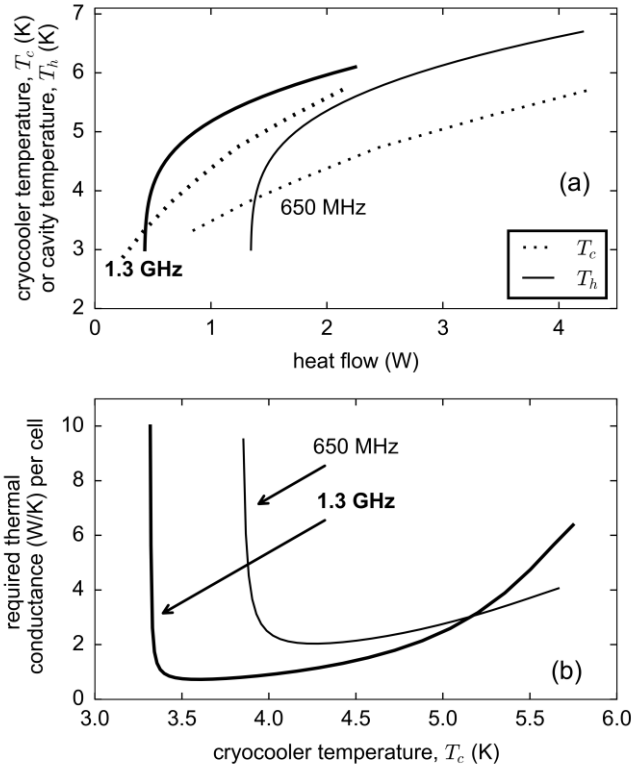

Fig. 2. Characteristics of cryocooler conduction-cooled SRF cavity (a) comparison of cavity and cryocooler operating temperatures for a given heat flow from the cavity to the cryocooler and (b) required thermal conductance between the cavity and the cryocooler for stable operation at a given cryocooler temperature.

In fact, such an analysis can tell the lowest cryocooler temperature sustainable for any given RF operating parameters.

The cryocooler operating temperature in the $T_h > T_c$ regime can be selected based on the link thermal conductance ($=Q_c(T_c)/(T_h-T_c)$) that is required for a given T_c. The plot of the required conductance *vs.* T_c in Fig. 2(b) reveals that both frequencies demand large conductance near the lowest allowed T_c, the conductance requirement relaxes as T_c rises, and again tightens for significantly warmer T_c. The T_c corresponding to the minimum required thermal conductance may be termed as the 'optimal' operating temperature of the cryocooler.

C. Link thermal design considerations

The curves in Fig. 2(b) represent the link design thermal conductance capable of supporting operation of the cryocooler-cavity system. Although a thermal link may be designed to sustain operation at optimal T_c, certain alternatives are worthwhile to consider. Imperfect Nb_3Sn coating conditions can produce local spots of off-stoichiometry Nb-Sn compounds on the RF surface with <<18 K transition temperature. There can even be uncoated spots where the RF surface is niobium with transition near 9 K. Both these situations can present significant BCS surface resistance near 4 K. Operation of the system as cold as possible in these scenarios can keep dissipation under the cooling budget. A link with large thermal conductance and operation at T_c much lower than the optimal can help to mitigate the effects of imperfect Nb_3Sn coating. To serve this purpose, a link should be designed on the steep portion of the conductance curve (Fig. 2(b)), which can support operation at lower than the optimal T_c.

If perfect coating can be established, the link may be designed with conductance on the near-flat portion of the conductance curve, *i.e.*, T_c warmer than optimal. Here, the system will be less sensitive to any unexpected static heat leak, due to higher cooling capacity of the warmer-operating cryocooler.

In the next section, we will design the thermal link such that its conductance lies on the steep part of the requirement curve. We will show that this design can also support operation in the presence of static heat load to the cryocooler.

TABLE II
DIMENSIONS OF THERMAL LINK COMPONENTS

Component	650 MHz	1.3 GHz
Nb ring*	ID=16, OD=18.5	ID=8, OD=10
Al ring*	ID=16, OD=18.5	ID=8, OD=10
Al ear-strap*	length=9, width=4.5	length=6, width=5
Al bus-bar**	length=9, width=4.5	length=4.5, width=5

*thickness=0.16, **thickness=0.375; all dimensions in inches.

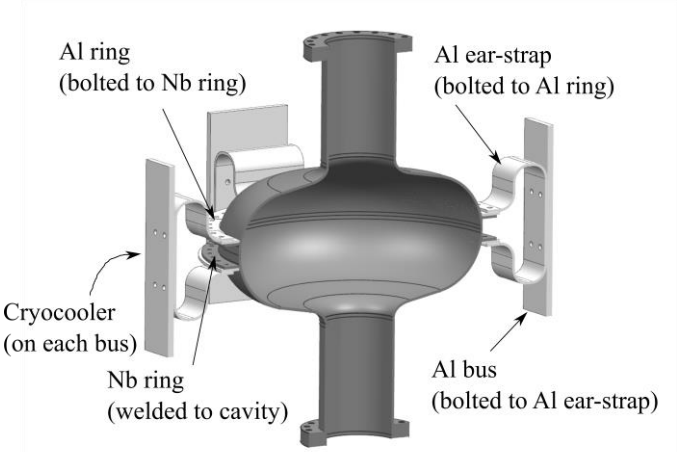

Fig. 3. CAD model of thermal link attached to the cavity. Going from the cavity to the cryocooler, the link has Nb rings welded to the cavity, Al rings bolted to the Nb rings, Al ear-straps bolted to the Al rings, and Al bus-bars bolted to the ear-straps. All bolted joints use thin film of indium as interposer. The thermal link is illustrated for a single cell cavity. For a multi-cell cavity, all the in-line ear-straps will connect to a bus-bar that will stretch across the cavity length.

III. CONDUCTION LINK DESIGN

A. Mechanical design and thermal properties

Magnetic field lines in a resonant cavity with the accelerating mode concentrate in the equatorial region of the elliptical cell. As a result, the majority of power is dissipated in the surface near the cell equator. Considering this fact our link is designed to attach to the cavity cell near its equator as depicted in Fig 3. Flat faces are machined on the cell outer wall where rings made of niobium (Nb) are welded to the cell. A thermal

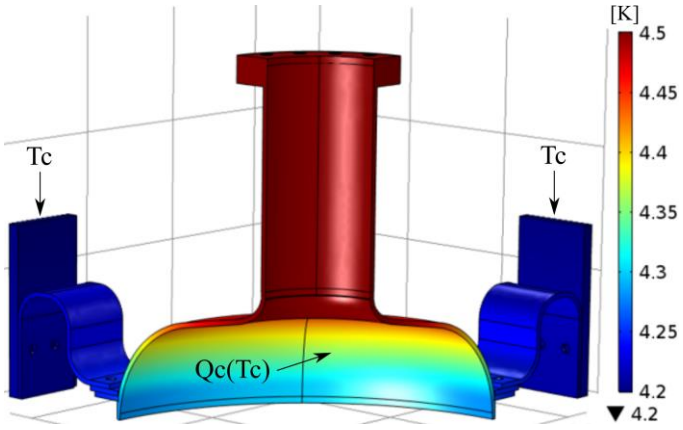

Fig. 4. Simulation geometry and steady state temperature distribution between the RF surface and the cryocooler interface of the thermal link. Due to symmetry, the thermal simulations used an octant of geometry of Fig. 3. Boundary conditions: constant T_c on the Al bus; heat flux $Q_c(T_c)$ on the RF surface. Heat flux divided by temperature difference between the RF surface and the cryocooler yielded the total thermal conductance. Sample result with 650 MHz cell and T_c = 4.2 K is shown while conductance at other temperatures were obtained by varying T_c and $Q_c(T_c)$.

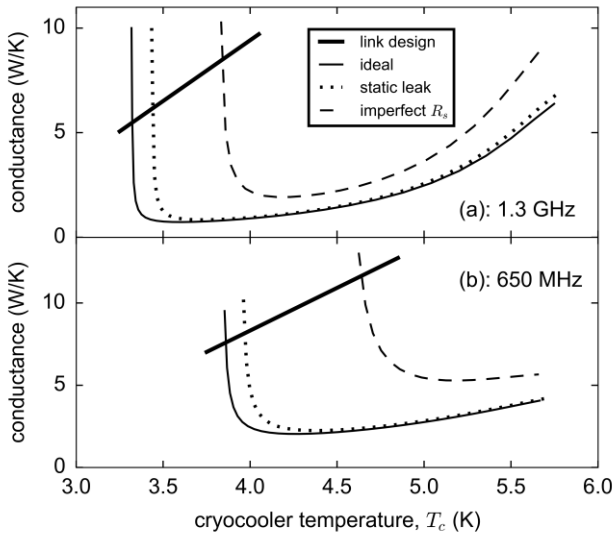

Fig. 5. Calculated link thermal conductance (bold solid line) and the required conductance for (a) 1.3 GHz and (b) 650 MHz cavity per cell. The required conductance is shown for ideal coating with no static load (solid line), static load (dotted line, 0.1 W for 650 MHz and 0.05 W for 1.3 GHz), and imperfect coating with 50% higher surface resistance (dash line). Intersection of thermal link conductance with the required conductance curve denotes the operating temperature in each case.

link made of high purity (5N) aluminum (Al) is then bolted to these niobium rings. The Al thermal link has three components: circular rings that bolt on to the niobium rings, slightly flexible ear-shape straps to accommodate differential thermal contraction during cooldown, and thick bus-bars that ultimately connect to the cryocoolers. Table II lists the thermal link dimensions.

The total link thermal conductance stems from bulk thermal conductivities of aluminum and niobium (rings plus cell walls), thermal conductance at bolted contacts of niobium-aluminum and aluminum-aluminum, and thermal resistance of the niobium-niobium weld. Fig. 1(c) shows material thermal conductivities of 5N Al and SRF grade Nb taken from [11] and [12]. Thermal resistance of bolted contacts [13] and welded contacts was measured in-house and is plotted with temperature in Fig. 1(d).

B. *Link thermal conductance*

Thermal simulations with COMSOL Multiphysics® Heat Transfer module yielded thermal conductance of the geometry of Fig. 3. In Fig. 4 we plot the steady state temperature distribution on an octant section with the bus-cryocooler interface held at cryocooler temperature T_c and a heat flow $Q_c(T_c)$ imposed on the RF surface. The overall thermal conductance between the RF surface and the cryocooler is equal to the heat flow divided by the temperature difference between the RF surface and cryocooler. The surface average temperature at the cell was used in the calculation. The sample result displayed in Fig. 4 is for the 650 MHz cell with T_c = 4.2 K and per-cell $Q_c(T_c)$ determined from the data in Fig. 1(b).

A parametric sweep in T_c gave the link thermal conductance over a wider range of operating temperatures. The link conductance so obtained is compared in Fig. 5 to the required conductance, wherein the point of intersection is the cryocooler operating temperature. For both the frequencies of 1.3 GHz (Fig. 5(a)) and 650 MHz (Fig. 5(b)), the link conductance curve crosses the steep part of the required conductance curve. The link therefore adheres to our criterion set in Section II(c), *i.e.*, the conductance is to be large enough to support relatively colder cavity-cryocooler operation.

We examine, although qualitative, two additional cases. First, we assume 0.05 W and 0.1 W static heat load per cell respectively to the 1.3 GHz and 650 MHz cells. Second, we assume that RF surface resistance is 50% higher than in Fig. 1(a). The dash and dash-dot lines represent the required thermal conductance for these 'non-ideal' cases. The imperfections add to the heat flow into the cryocooler and cause the cryocooler to operate warmer than in the ideal case. Fortunately, the link thermal conductance rises with temperature because of improvement in both material thermal conductivity and joint thermal resistance. With the current design, the link conductance curve intersects the required conductance lines for both the non-ideal cases, indicating that the link can support operation even when there is static heat leak or imperfect coating. Cases with other static loads or imperfect coatings can be analyzed in a similar way.

IV. SUMMARY

Using surface heat dissipation in cavities and cooling power of a commercial cryocooler, we analyzed the thermal behavior of a cryogen-free conduction-cooled SRF system. The thermal conductance requirement of the link connecting the cavity to the cryocooler was identified for qualitative cases with static heat load and imperfect Nb_3Sn coating. A simple-to-construct conduction link design is described, which can support the cavity operation in all of the cases considered.

REFERENCES

[1] S. Posen and D. L. Hall, "Nb_3Sn superconducting radiofrequency cavities: fabrication, results, properties, and prospects," *Supercond. Sci. Technol.*, vol. 30, Art. No. 033004, 2017.

[2] R. Kephart, "Conduction cooling systems for linear accelerator cavities," *US Patent 9642239 B2*, May 2, 2017.

[3] R. Kephart et al., "SRF, compact accelerators for industry & society," in *Proc. SRF2015*, pp. 1467-1473, 2015.

[4] R. Kostin et al., "operation regime analysis of conduction cooled cavities through multi-physics simulation," in *Proc. IPAC2018*, pp. 2697-2699, 2018.

[5] J.P. Holzbauer and A. Nassiri, "Thermal study of a cryogen-less MgB_2 cavity," *Nuclear Instruments and Methods in Physics Research A*, vol. 767, pp. 407-414, 2014.

[6] A. Nassiri et al., "Cryogen-free RF system studies using cryocooler-cooled Magnesium Diboride-coated copper RF cavities," in *Proc. SRF2013*, pp. 663-665, 2013.

[7] G. Ciovati et al., "Design of a cw, low energy, high power superconducting linac for environmental applications," *Phys. Rev. Accel. Beams*, vol. 21, Art. No. 091601, 2018.

[8] B. Aune et al., "The Superconducting TESLA Cavities," Phys. Rev. ST Accel. Beams, vol. 3, Art. No. 092001, 2000.

[9] V. K. Jain et al., "650 MHz elliptical superconducting RF Cavities for PIP-II project," in *Proc. NAPAC2016*, pp. 859-862, 2016.

[10] SRIMP code available online at https://www.classe.cornell.edu/~liepe/webpage/researchsrimp.html (accessed Aug 28, 2018).

[11] A. L. Woodcraft, "Recommended values for the thermal conductivity of aluminium of different purities in the cryogenic to room temperature range, and a comparison with copper," *Cryogenics*, vol. 45, pp. 626–636 2005.

[12] F. Koechlin and B. Bonin, "Parametrization of the niobium thermal conductivity in the superconducting state," *Supercond. Sci. Technol.,* vol. 9, no. 6, pp. 453-457, 1996.

[13] R. C. Dhuley, M. I. Geelhoed, and J. C. T. Thangaraj, "Thermal resistance of pressed contacts of aluminum and niobium at liquid helium temperatures," *Cryogenics*, vol. 93, pp. 86-93, 2018.

[14] Cryomech PT420 specification sheet, available online at http://www.cryomech.com/cryorefrigerators/pulse-tube/pt420/ (accessed Aug 28, 2018).